

NASA TECHNICAL NOTE



NASA TN D-7738

NASA TN D-7738

(NASA-TN-D-7738) TORNADOLIKE
GRAVITY-DRIVEN VORTEX MODEL (NASA)
HC \$3.00

21 p
CSCL 20D

N74-30050

Unclas
45372

H1/20



TORNADOLIKE GRAVITY-DRIVEN VORTEX MODEL

by Robert G. Deissler and Donald R. Boldman

Lewis Research Center

Cleveland, Ohio 44135



NATIONAL AERONAUTICS AND SPACE ADMINISTRATION • WASHINGTON, D. C. • AUGUST 1974

1. Report No. NASA TND-7738	2. Government Accession No.	3. Recipient's Catalog No.	
4. Title and Subtitle TORNADOLIKE GRAVITY-DRIVEN VORTEX MODEL		5. Report Date August 1974	6. Performing Organization Code
		8. Performing Organization Report No. E-7917	
7. Author(s) Robert G. Deissler and Donald R. Boldman		10. Work Unit No. 502-04	11. Contract or Grant No.
9. Performing Organization Name and Address Lewis Research Center National Aeronautics and Space Administration Cleveland, Ohio 44135		13. Type of Report and Period Covered Technical Note	
		14. Sponsoring Agency Code	
12. Sponsoring Agency Name and Address National Aeronautics and Space Administration Washington, D. C. 20546		15. Supplementary Notes	
16. Abstract <p>A study was made of the buoyancy-induced vorticity concentration produced as the fluid in a vortex accelerates vertically. The boiloff from liquid nitrogen, to which a small amount of initial vorticity was added, provided a source of cool, heavy gas in which a concentration of vorticity could take place. Condensation streamers made the flow visible. It was shown that the presence of a surface boundary layer is not necessary for an effective concentration of vorticity. A simple theoretical analysis of the phenomenon was also made. A radial contraction of the flow with vertical position and a characteristic hook shape in the top view of the streamlines were observed in both theory and experiment. The vorticity concentration observed herein may be similar to that which occurs in tornadoes.</p>			
17. Key Words (Suggested by Author(s)) Tornado; Vortex; Buoyancy; Fluid mechanics		18. Distribution Statement Unclassified - unlimited Category 20	
19. Security Classif. (of this report) Unclassified	20. Security Classif. (of this page) Unclassified	21. No. of Pages 21	22. Price* \$3.00

* For sale by the National Technical Information Service, Springfield, Virginia 22151

TORNADOLIKE GRAVITY-DRIVEN VORTEX MODEL

by Robert G. Deissler and Donald R. Boldman

Lewis Research Center

SUMMARY

A study was made of the buoyancy-induced vorticity concentration produced as the fluid in a vortex accelerates vertically. The boiloff from liquid nitrogen, to which a small amount of initial vorticity was added, provided a source of cool, heavy gas in which a concentration of vorticity could take place. Condensation streamers made the flow visible. It was shown that the presence of a surface boundary layer is not necessary for an effective concentration of vorticity. A simple theoretical analysis of the phenomenon was also made. A radial contraction of the flow with vertical position and a characteristic hook shape in the top view of the streamlines were observed in both theory and experiment. The vorticity concentration observed herein may be similar to that which occurs in tornadoes.

INTRODUCTION

Although observations of tornadoes have been made for many years (the first known photograph of a tornado cloud was taken in 1884, ref. 1), there appears to be little general agreement about their mechanics. The lack of agreement is, of course, at least partly due to the devastating nature of tornadoes and the consequent difficulty of making meaningful measurements. Thus, theories and laboratory experiments should play an important role in tornado research.

Tornadoes nearly always occur in an unstable environment, with a cool air mass above a warm one (ref. 2), and it is generally thought that buoyancy effects are important in their formation. In addition, since large tangential velocities are present in tornadoes, a source of vorticity, such as a rotating cloud (ref. 3), must be present. Evidently, the vertical velocities induced by buoyancy effects cause radial inflow, which in turn concentrates the vorticity and produces the high tangential velocities associated with tornadoes.

The vertical velocities produced by an unstable environment could be either positive or negative, depending mostly on how the flow was started. Rossman (ref. 4), Hoecker (ref. 5), and others have concluded that the flow is generally upward in the outer portions of the vortex and downward in the core. The downflow might be started by rain or hail falling into a dry region where evaporative cooling could take place (refs. 6 and 7).

In this study we consider the concentration of vorticity by the inflow of a heavy, cool air mass (heavier than the surrounding air) accelerating downward. That is, vorticity at some height is convected downward as it is being concentrated. No claim that the vertical flow in an actual tornado is primarily downward, or that low-altitude vorticity is absent, is intended here. In fact, we could alternatively consider the concentration of vorticity by the inflow of a light, warm air mass accelerating upward. With slight modifications, essentially the same mechanism would evidently apply in either case. Both cases may occur simultaneously, as mentioned earlier. However, the assumption that vorticity is convected downward from above appears to explain the common observation that the parent cloud aloft rotates rapidly before effects are felt at the ground (ref. 8). Moreover, rotating funnel clouds often occur aloft but never affect the ground (ref. 9). Also, tornadoes are observed to be cold (ref. 6), indicating that cool air has descended from above.

The model considered herein, which may apply to a tornado in which downflows are present, considers what occurs before effects are felt at the ground. Although we are concerned with a downward flow of a cool air mass, there may be an upward flow of warm air above it in the tornado parent cloud (ref. 3). This would assure by continuity, a radial inflow, particularly near the interface between the warm and cool regions, which could concentrate the vorticity.

It might be mentioned that effects other than those due to buoyancy probably affect the concentration of vorticity in a tornado. In particular, axial stretching of the tornado (or vortex filament) by vertical wind shear can produce vorticity concentration. This stretching of the vortex filament by a mean velocity gradient may be similar to that which occurs for the random vortex filaments in a turbulent shear flow (ref. 10).

In the experiment described herein, the boiloff from liquid nitrogen is used as a source of cool gas made visible by condensation from the atmosphere. First, however, an analysis of buoyancy-induced vorticity concentration is given.

ANALYSIS

We consider here a simple model which illustrates how acceleration produced by buoyancy can cause a concentration of vorticity. Friction is neglected, and it is assumed that the density depends effectively only on temperature and is only moderately

removed from its equilibrium value. Then the steady-state equations for the conservation of mass and momentum for an axially symmetric flow can be written as (ref. 11).

$$\frac{1}{r} \frac{\partial}{\partial r} (ru) + \frac{\partial w}{\partial z} = 0 \quad (1)$$

$$w \frac{\partial w}{\partial z} + u \frac{\partial w}{\partial r} = - \frac{1}{\rho} \frac{\partial(p - p_e)}{\partial z} + \beta g(T - T_e) \quad (2)$$

$$u \frac{\partial v}{\partial r} + w \frac{\partial v}{\partial z} + \frac{uv}{r} = 0 \quad (3)$$

and

$$u \frac{\partial u}{\partial r} + w \frac{\partial u}{\partial z} - \frac{v^2}{r} = - \frac{1}{\rho} \frac{\partial(p - p_e)}{\partial r} \quad (4)$$

where r and z are, respectively, the radial and vertical coordinates; u , v , and w are, respectively, the radial, tangential, and vertical velocities; ρ is the density; p is the pressure; T is the temperature; p_e and T_e are, respectively, the equilibrium pressure and temperature; g is the acceleration of gravity; and β is the thermal expansion coefficient given by

$$\beta = - \frac{1}{\rho} \left(\frac{\partial \rho}{\partial T} \right)_p \quad (5)$$

The last term in equation (2) is the buoyancy term. Let $w = w(z)$ and $v = v(r)$ within the vortex, or the region of interest. If the first two terms in equation (4) are small compared with the third term, as they probably are for a tornado (ref. 5), equation (4) shows that $p = p(r)$. Equations (1) to (3) become

$$\frac{1}{r} \frac{\partial}{\partial r} (ru) + \frac{\partial w(z)}{\partial z} = 0 \quad (6)$$

$$w \frac{\partial w(z)}{\partial z} = \beta g(T - T_e) \quad (7)$$

and

$$\frac{\partial v(r)}{\partial r} + \frac{v(r)}{r} = 0 \quad (8)$$

We assume now that the buoyancy term $\beta g(T - T_e)$ is constant throughout the vortex. Solution of equation (7) with the initial condition $w = 0$ when $z = 0$ then gives

$$w = \pm \left[2\beta g(T - T_e)z \right]^{1/2} \quad (9)$$

From equations (6) and (9) we get, by using the condition that u is finite at $r = 0$,

$$u = \mp \frac{\left[2\beta g(T - T_e)z \right]^{1/2} r}{4z} \quad (10)$$

Along a streamline,

$$\frac{u}{w} = \frac{dr}{dz} = - \frac{1}{4} \frac{r}{z} \quad (11)$$

or

$$\frac{r}{r_i} = \left(\frac{z}{z_i} \right)^{-1/4} \quad (12)$$

That is, for the model considered herein the radius at a particular streamline within the vortex varies as $z^{-1/4}$. The quantity z_i is the value of z at some inner reference radius r_i .

From equation (8) we get

$$\frac{v}{v_i} = \left(\frac{r}{r_i} \right)^{-1} \quad (13)$$

where v_i is the tangential velocity at $r = r_i$. This equation applies reasonably well except for small r , where friction may become important (ref. 12). From equations (12) and (13) we get

$$\frac{v}{v_i} = \left(\frac{z}{z_i}\right)^{1/4} \quad (14)$$

Equation (14) gives the variation of v with z along a streamline within the vortex.

Equations (12) and (14) apply when the vertical flow is either upward or downward, depending on whether the temperature in the vortex is higher or lower than that in the surrounding fluid. They are plotted for downflow in figure 1. As expected, the largest variations of r and v with z along a streamline take place near $z = 0$.

APPARATUS AND PROCEDURE

The apparatus is illustrated in figure 2. The cup of boiling liquid nitrogen provides a source of cool (heavy) gas which becomes visible because of condensation from the atmosphere. The temperature of the gas in the vortex emerging from the hole in the bottom of the container was typically about 30° C below the atmospheric temperature $((T - T_e)/T_e \approx -0.1)$.

The heavy gas from the cup flowed down the space between the insulated cylindrical container and the smaller hollow clear-plastic cylinder. It then flowed nearly radially across the gap between the bottom of the container and the bottom of the smaller cylinder and accelerated downward as it flowed out of the hole in the container. The smaller cylinder had a diameter slightly larger than that of the hole in the container and was open at the bottom but closed at the top, so that vorticity concentration could take place in a region without a surface boundary layer. The gas in the container was given a small amount of initial vorticity by auxiliary gas which entered the container tangentially through a nozzle. The heavy gas swirled inward to a radius considerably smaller than that of the hole in the container and had an outline similar to that shown in figure 1. Before photographs were taken, the cup of liquid nitrogen was removed from the container, and the gas from the tangential nozzle was turned off. That procedure gave a smooth, visible vortex flow, particularly after the condensation had dissipated to some extent. At that stage, most of the radial flow was produced by the downward acceleration of the heavy gas leaving the container. Still pictures were taken every 3 seconds using a motorized single-lens-reflex camera. A few motion pictures were also taken.

This arrangement of the test apparatus was used in order to give a vertical velocity which was essentially zero at some horizontal plane $z = 0$ (near the top of the gap where the flow entered nearly radially), as assumed for the initial condition in the section ANALYSIS. In an actual parent cloud above a tornado, that condition might be attained by a layer of upward-moving warm air above the layer of downward-moving cool air.

However, experimentally, it was easier to use the arrangement described herein. Closing the cylinder at its top instead of at its bottom produced the desired essentially zero vertical velocity near the top of the gap where the flow entered the vortex without producing a surface boundary layer there.

A few runs were also made with a horizontal plate at the top of the gap where the fluid entered the vortex. Then, if we imagine that the configuration is inverted, the flow should simulate the vorticity concentration produced by a radial and vertical flow of warm air near the ground.

RESULTS AND DISCUSSION

Gravity-driven vortexes are shown in figures 3 to 5. Figure 6 shows the flow in the apparatus without swirl and is included for comparison with figure 3. As mentioned in the section APPARATUS AND PROCEDURE, the cup of liquid nitrogen was removed and the source of initial vorticity was turned off before photographs were taken. Most of the photographs were taken after the condensation cloud had dissipated to some extent (beginning at time = 0). That procedure gave the best flow visualization and ensured that most of the flow was produced by the downward acceleration of the heavy gas leaving the container, rather than by the hydrostatic head of the entering gas. The top, bottom, and the lower side views (figs. 3 to 5) indicate that the gas flowed inward to a radius considerably smaller than that of the hole in the bottom of the container and that a strong concentration of vorticity took place during the radial inflow. The top views are particularly striking, indicating that the horizontal component of the velocity vector changes from nearly radial at the edge of the hole to nearly tangential near the center. The condensation streamers appear to be very effective in rendering the flow visible. They seem to form a characteristic hook shape as they spiral toward the center. The denseness of the condensation near the center is due to the column of gas flowing nearly vertically beneath the plane of the hole in the container.

The contraction of the stream as it accelerates downward is shown typically by the lower side views in figure 5. The shape of the profile appears to be similar to that predicted in figure 1, at least for the region reasonably near the top. As the flow continues downward, friction and heat-transfer effects appear to become important, and the vortex begins to dissipate. The quickness of the dissipation of the vortex is evidently related to its smallness. Because of the much larger size of tornadoes, frictional and heat-transfer effects may be less important in tornadoes.

The photographs in figures 3 to 5 were made using the configuration shown in figure 2. As mentioned in the last section, the flow in this vortex should be somewhat similar to that in a vortex which might descend from a tornado parent cloud, in which

no surface boundary layer is present. (Radial inflow may be ensured by an upflow of warm air over the cool descending air.) On the other hand, if we wish to consider a possible concentration of vorticity by radial inflow of warm air over the ground, we might place a horizontal plate over the vortex region where the inflow occurs and then imagine that the apparatus is inverted. A horizontal plate was placed over the vortex region for the photographs shown in figure 7. Visually, the flow seems to be much the same as that in figure 3; that is, the presence of the boundary layer at the plate (or ground) does not seem to produce a first-order effect. As in figures 3 and 4, the hook shape of the streamlines is evident.

Although the appearance of the swirl with and without the horizontal surface is similar, the vertical profile of the radial velocity may be different in the two cases. In the presence of the horizontal surface the radial flow may take place in a thin layer near the surface, since centrifugal effects are less there (teacup effect). However, the presence of a surface is not necessary for an effective concentration of vorticity, as shown in figure 3.

The hook shape of the streamlines in figures 3, 4, and 7 can be predicted by using the equations in the section ANALYSIS. Along a streamline,

$$\frac{v}{u} = \frac{r}{dr} \frac{d\theta}{dr} \quad (15)$$

Substituting the expressions for u and v from equations (10) and (13), eliminating z by equation (12), and integrating give, for the relation between r and θ along a streamline,

$$\theta = \theta_i \frac{\left(\frac{r}{r_0}\right)^{-4} - 1}{\left(\frac{r_i}{r_0}\right)^{-4} - 1} \quad (16)$$

where θ was set equal to 0 at the outer radius r_0 , and θ_i is the value of θ at an inner reference radius r_i . Equation (16) is plotted in figure 8, where the similarity to the hook-shaped streamlines in figures 3, 4, and 7 is evident.

Motion pictures were also taken of the flow shown in figures 3 to 5 and were used in an attempt to obtain the radial variation of tangential velocity (fig. 9). Except near the center of the vortex, v tends to follow the r^{-1} variation predicted by equation (13). The data points at $r/r_0 = 0.3$ lie below the r^{-1} curve because the effects of friction

become important near the center. At $r = 0$, v goes to zero (ref. 12). The square data point at $r/r_0 = 0.7$ is probably too low.

CONCLUDING REMARKS

An experimental gravity-driven vortex model had features which may be similar to those occurring in tornadoes. In particular, a strong concentration of vorticity was produced by vertical accelerations and radial inflow without a surface boundary layer. This type of vorticity concentration may occur in a tornado parent cloud.

The horizontal component of the velocity changed from nearly radial to nearly tangential as the fluid spiraled toward the center of the vortex. Condensation streamers were effective in rendering the cool gas (boiloff from liquid nitrogen) visible. They appeared to form a characteristic hook shape as they spiraled toward the center. The tangential velocity varied inversely as the first power of the radius except near the center of the vortex, as expected.

Although most of the study was made with a cold swirling mass of gas accelerating downward, a similar vorticity concentration would evidently occur in a warm mass of gas accelerating upward from the ground. That case was studied by placing a plate (simulating the ground) at the top of the vortex and imagining the apparatus to be inverted. The results were similar to those without the plate.

A simple theoretical analysis of a vortex flow indicated tangential velocities and a radial contraction of the vortex as it accelerated vertically which were similar to those in the experiments. The characteristic hook shape of the experimental streamlines (shown in the top views) was also predicted by the analysis.

In addition to the buoyancy effects, which were the main consideration in this study, other effects such as the axial stretching of the vortex by horizontal wind shear may play an important role in the concentration of vorticity in a tornado.

Lewis Research Center,
National Aeronautics and Space Administration,
Cleveland, Ohio, May 8, 1974,
502-04.

REFERENCES

1. Science, vol. 176, no. 4042, June 30, 1972, cover.
2. Tepper, Morris: Tornadoes. Sci. Amer., vol. 198, no. 5, May 1958, pp. 31-37.

3. Fugita, T.: Mother Cloud of the Fargo Tornadoes of 20 June, 1957. In *Cumulus Dynamics*, C. E. Anderson, ed., Pergamon Press (New York), 1960, pp. 175-177.
4. Rossman, F. O.: On the Physics of Tornadoes. In *Cumulus Dynamics*, C. E. Anderson, ed., Pergamon Press (New York), 1960, pp. 167-174.
5. Hoecker, W. H., Jr.: Three-Dimensional Pressure Pattern of the Dallas Tornado and Some Resultant Implications. *Monthly Weather Rev.*, vol. 89, no. 12, Dec. 1961, pp. 533-542.
6. Brooks, E. M.: Tornadoes and Related Phenomena. In *Compendium of Meteorology*, T. F. Malone, ed., Amer. Meteorological Soc. (Boston), 1951, pp. 673-680.
7. Miller, J. A.: Dry Air Intrusion into A Low-Level Moist Tongue As Viewed by ATS-3. *Monthly Weather Rev.*, vol. 101, July 1973, pp. 594-595.
8. Browning, K. A.: The Evolution of Tornadic Storms. *J. Atmos. Sciences*, vol. 22, Nov. 1965, pp. 664-668.
9. Modahl, A. C.; and Gray, W. M.: Summary of Funnel Cloud Occurrences and Comparison with Tornadoes. *Monthly Weather Review*, vol. 99, no. 11, Nov. 1971, pp. 877-882.
10. Deissler, R. G.: Direction of Maximum Turbulent Vorticity in a Shear Flow. *Phys. Fluids*, vol. 12, no. 2, Feb. 1969, pp. 426-427.
11. Landau, Leo D.; and Lifshitz, E. M.: *Fluid Mechanics*. Pergamon Press, 1959, p. 212.
12. Deissler, R. G.; and Perlmutter, M.: Analysis of the Flow and Energy Separation in a Turbulent Vortex. *Int. J. Heat Mass Transfer*, vol. 1, no. 2/3, Aug. 1960, pp. 173-191.

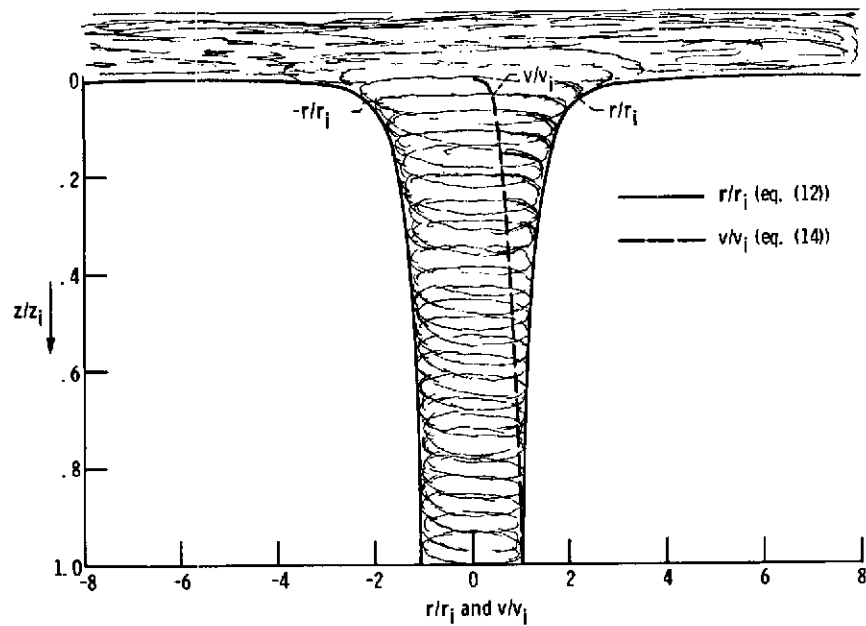


Figure 1. - Predicted variations, with vertical distance, of radius and tangential velocity along a streamline.

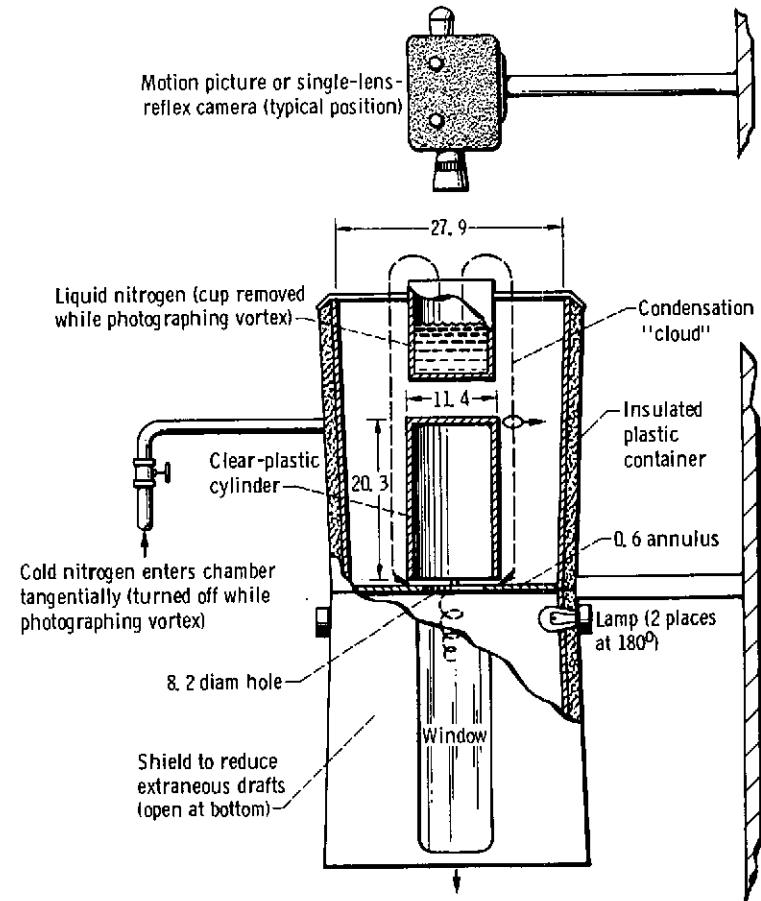
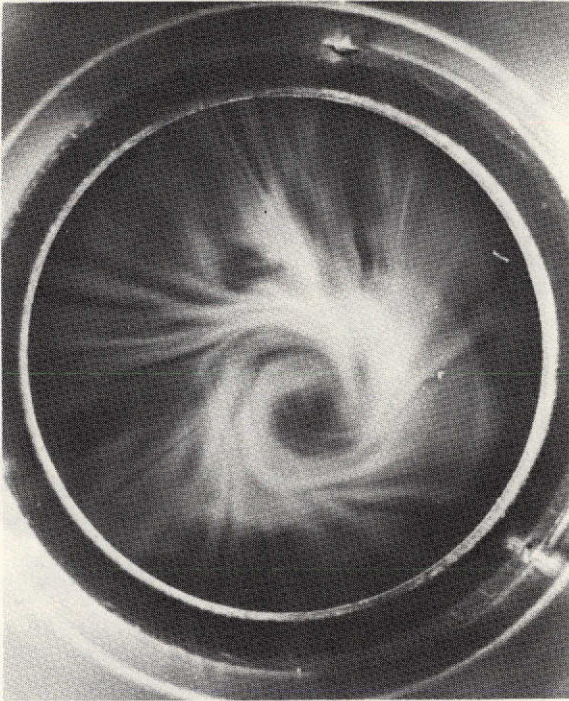
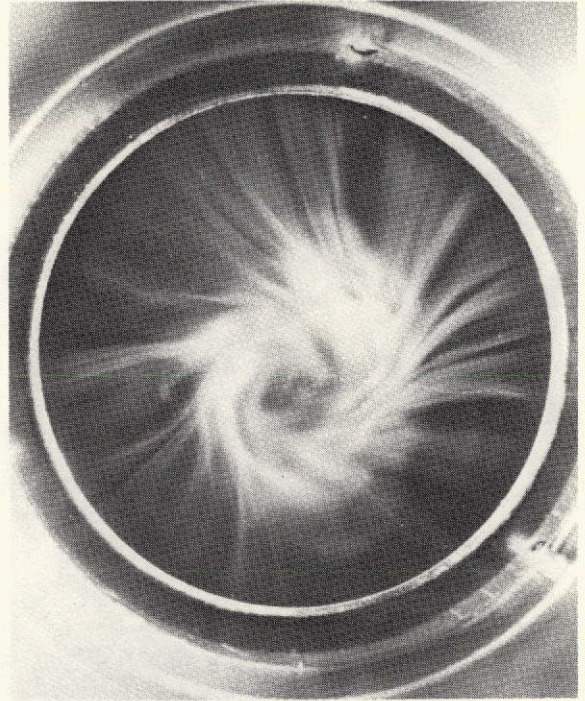


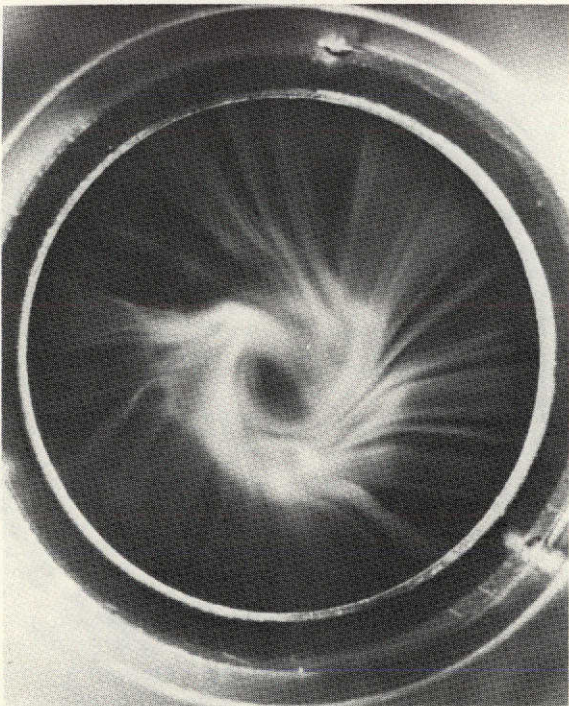
Figure 2. - Apparatus for observing vortex flow. (All dimensions are in cm.)



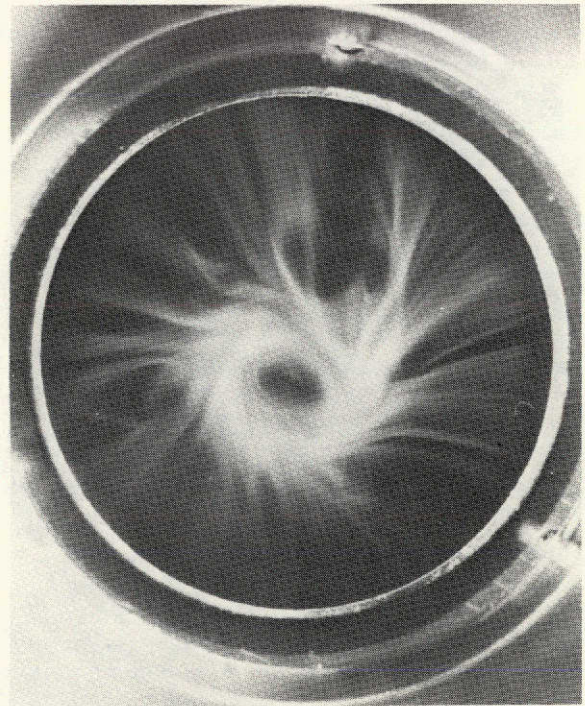
(a) Sequence 1; time, 0 second.



(b) Sequence 1; time, $\frac{2}{3}$ second.

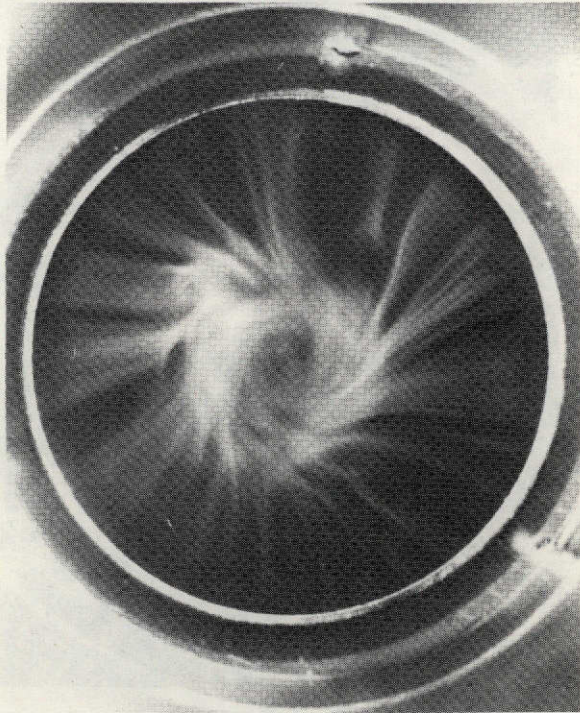


(c) Sequence 1; time, 1 second.

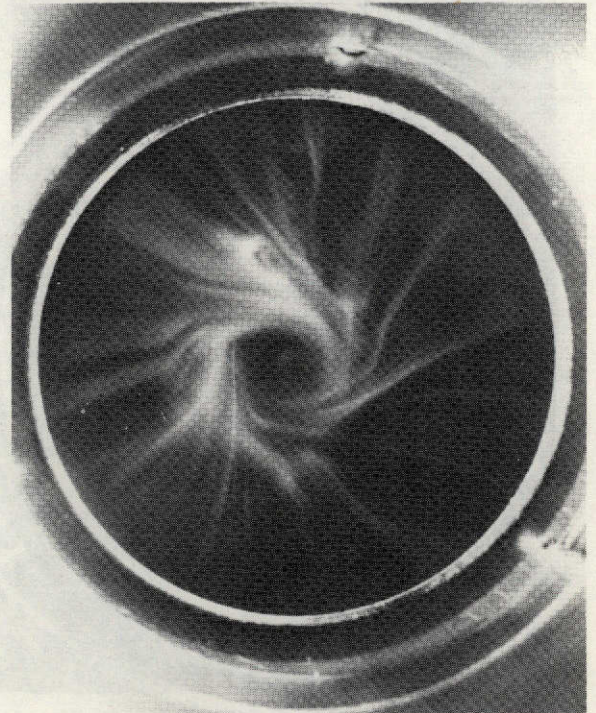


(d) Sequence 1; time, $1\frac{1}{3}$ seconds.

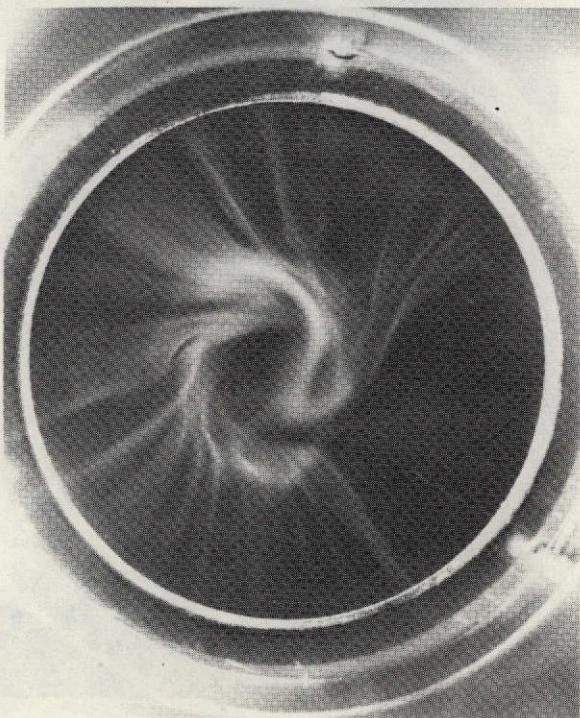
Figure 3. - Top views of vortices observed in apparatus of figure 2.



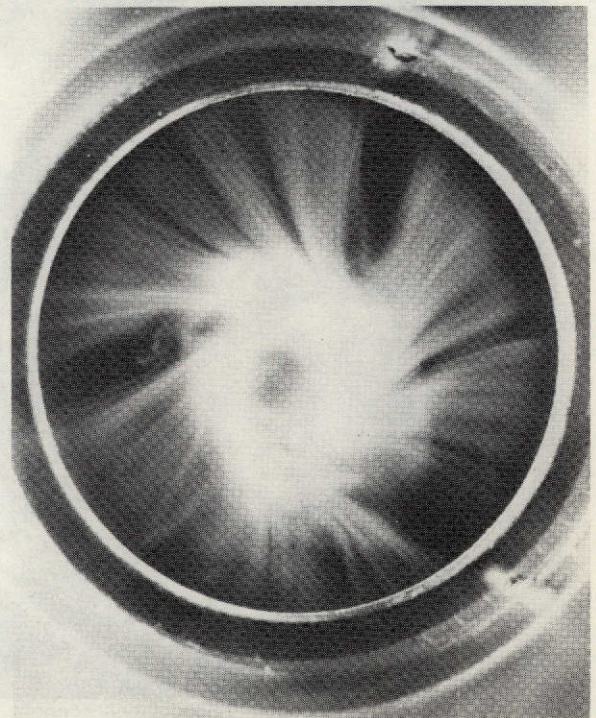
(e) Sequence 1; time, $1\frac{2}{3}$ seconds.



(f) Sequence 1; time, 2 seconds.

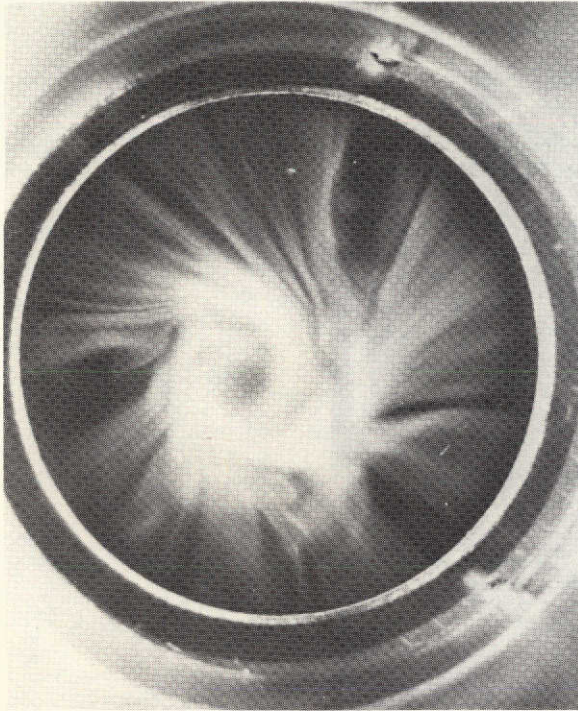


(g) Sequence 1; time, $2\frac{1}{3}$ seconds.

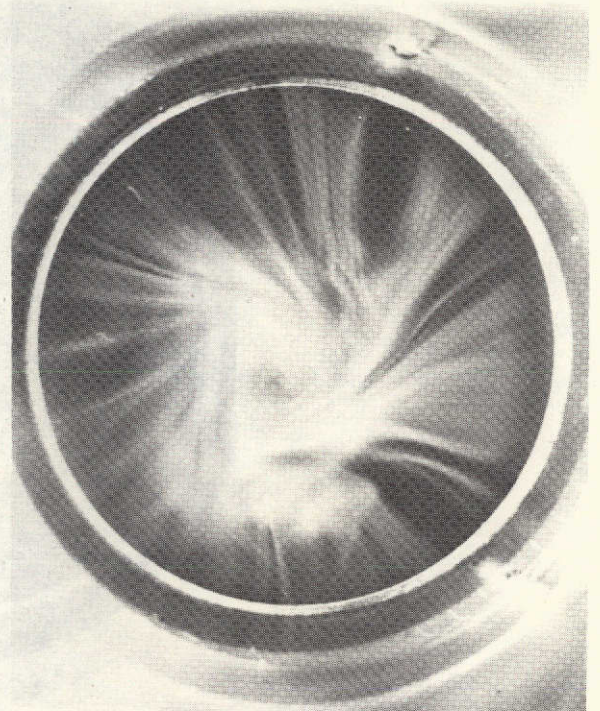


(h) Sequence 2; time, 0 second.

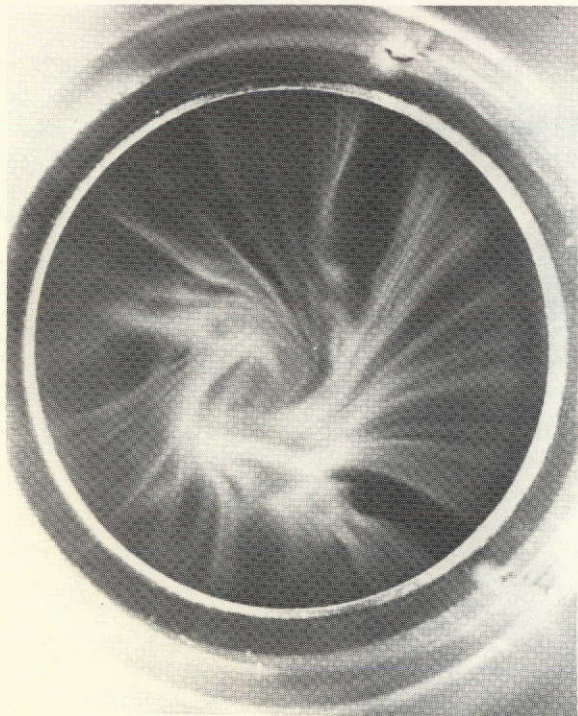
Figure 3. - Continued.



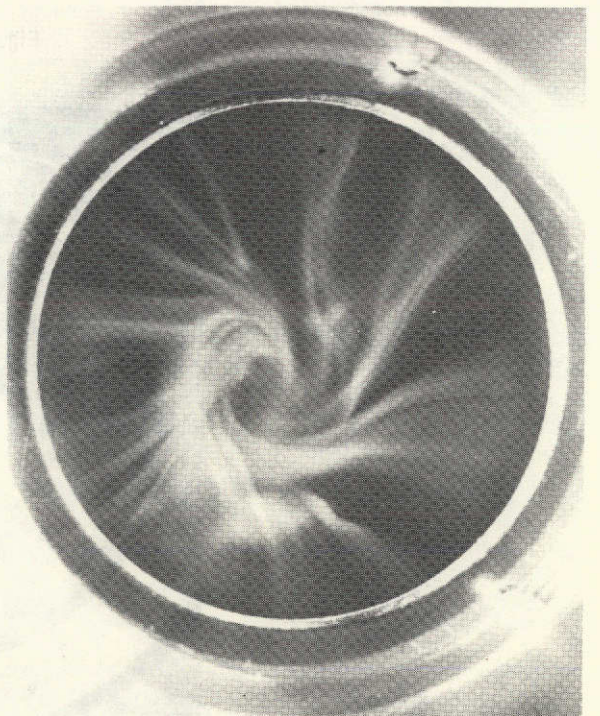
(i) Sequence 2; time, $1/3$ second.



(j) Sequence 2; time, $2/3$ second.

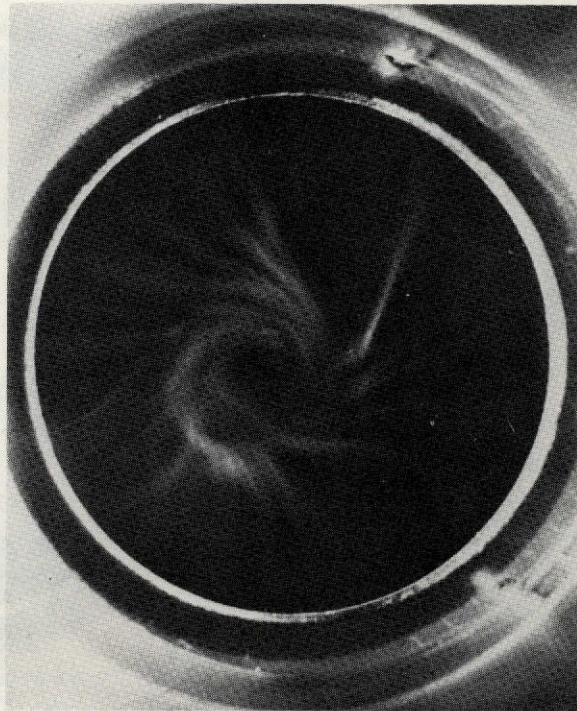


(k) Sequence 2; time, 1 second.



(l) Sequence 2; time, $1\frac{1}{3}$ seconds.

Figure 3. - Continued.



(m) Sequence 2; time, $1\frac{2}{3}$ seconds.

Figure 3. - Concluded.

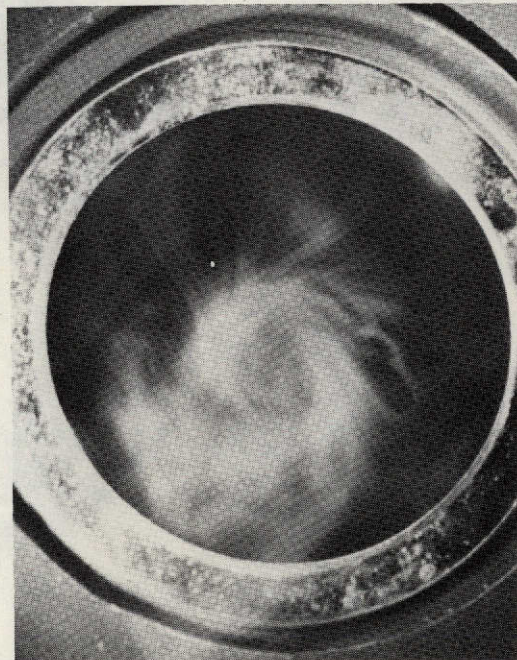
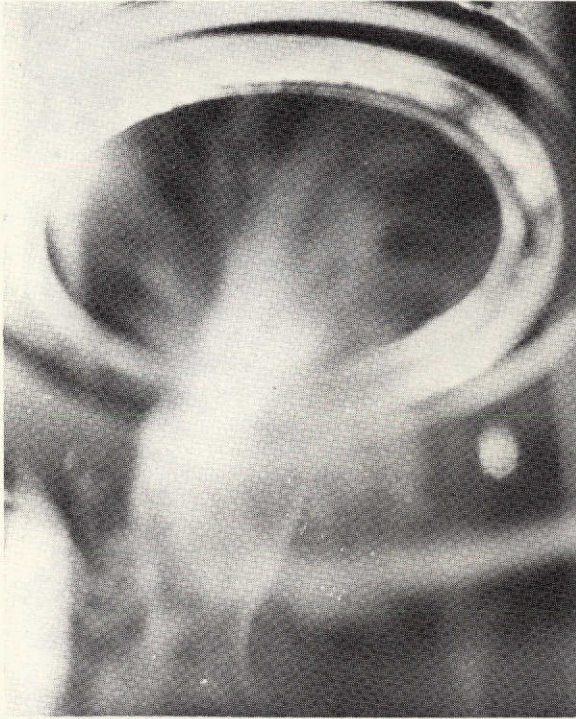
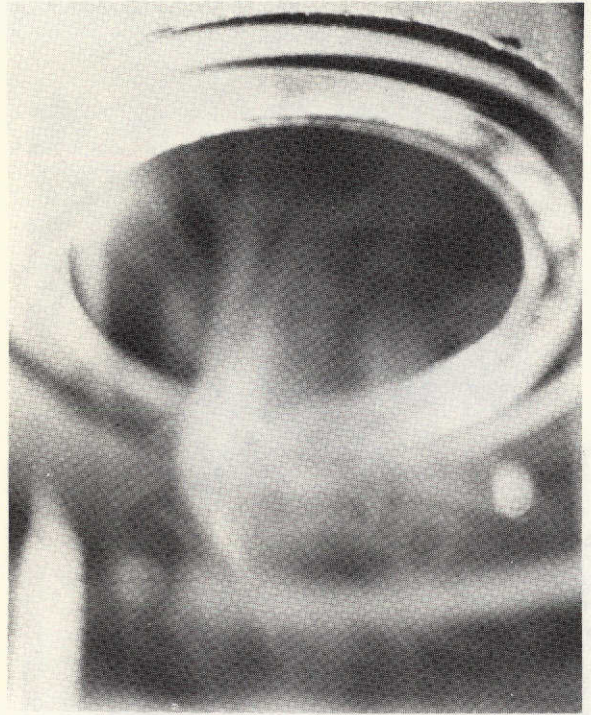


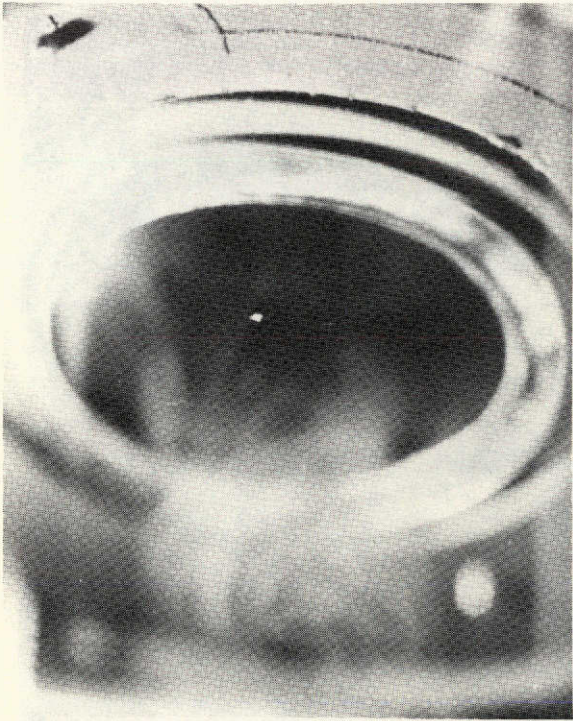
Figure 4. - Bottom view of vortex observed in apparatus of figure 2.



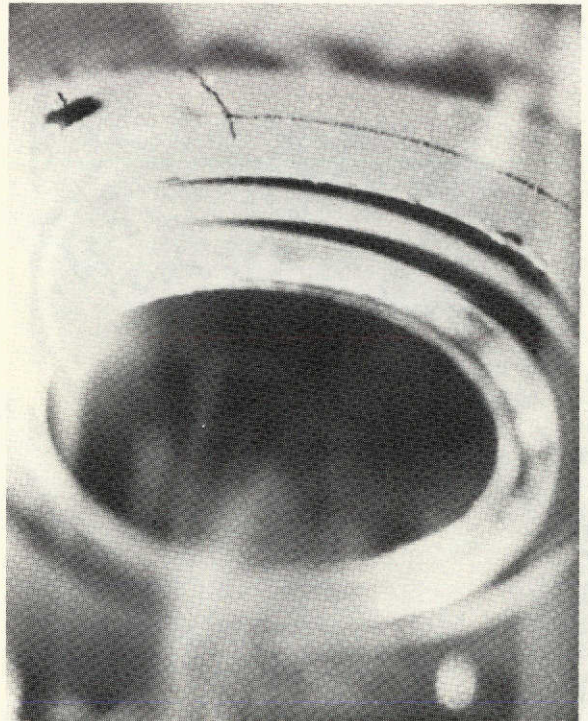
(a) Sequence 1; time, 0 second.



(b) Sequence 1; time, $2\frac{1}{3}$ seconds.

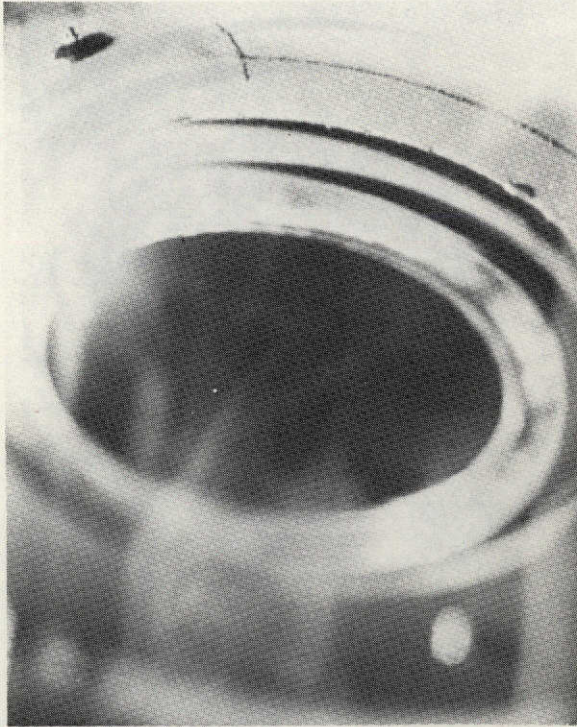


(c) Sequence 1; time, 3 seconds.

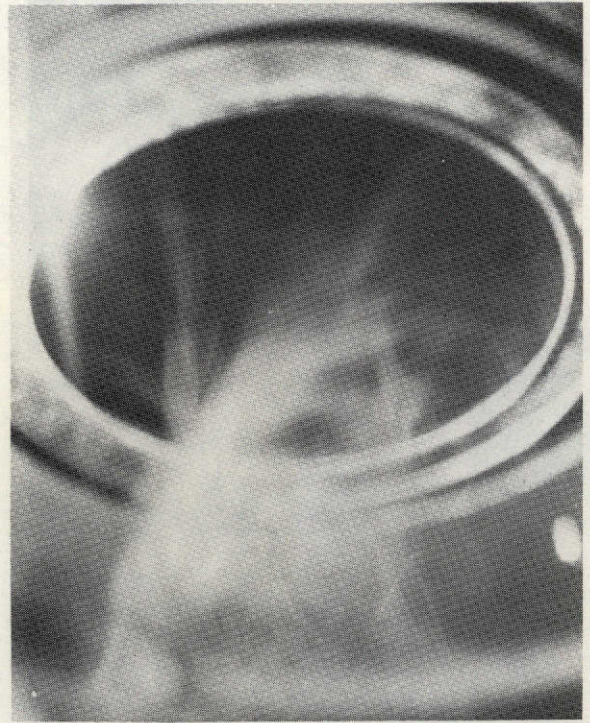


(d) Sequence 1; time, $3\frac{1}{3}$ seconds.

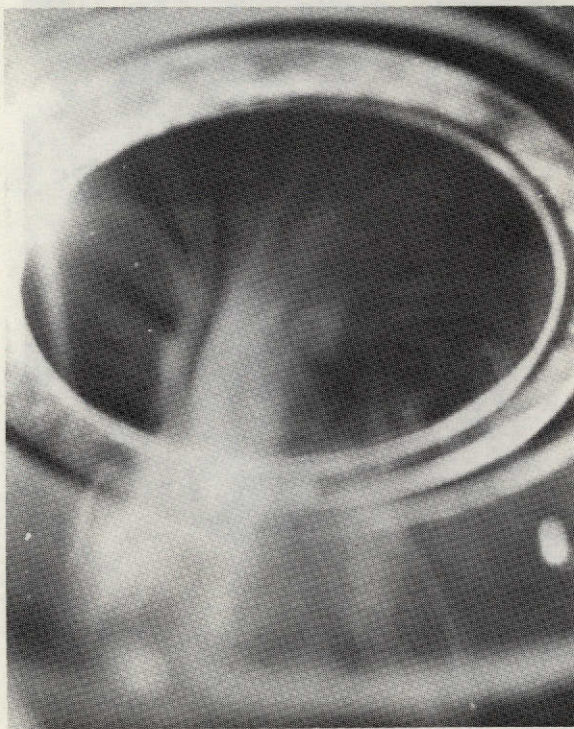
Figure 5. - Lower side views of vortexes observed in apparatus of figure 2.



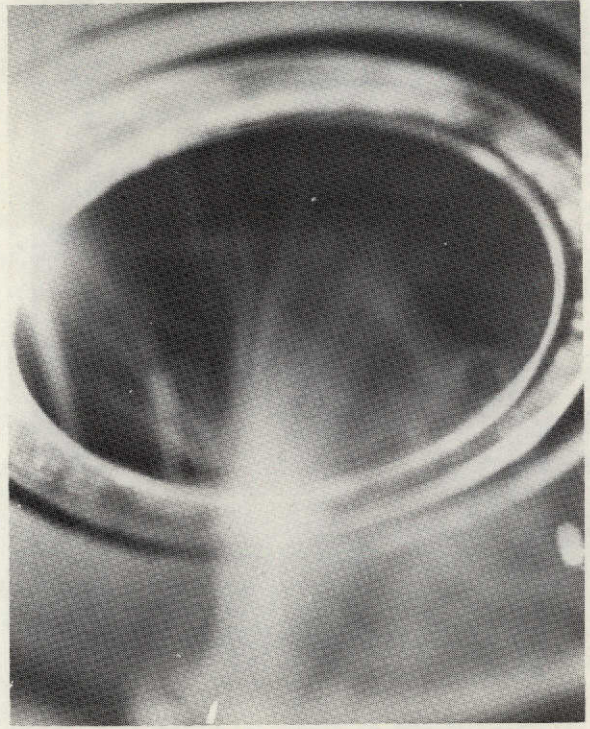
(e) Sequence 1; time, $3\frac{2}{3}$ seconds.



(f) Sequence 2; time, 0 second.



(g) Sequence 2; time, $1/3$ second.



(h) Sequence 3; time, 0 second.

Figure 5. - Concluded.

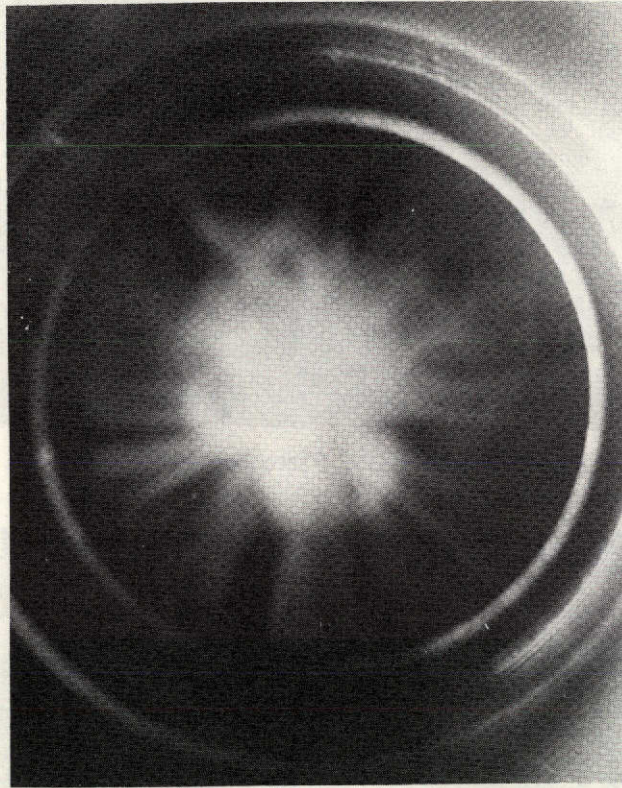
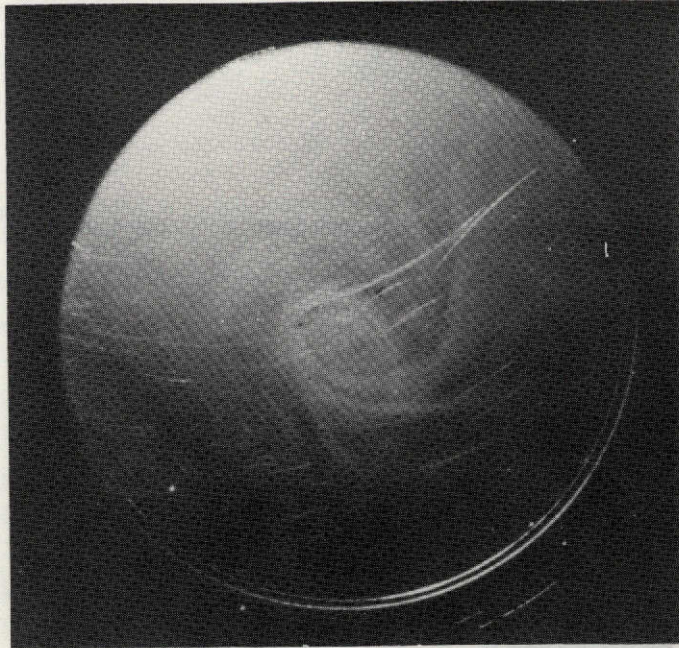
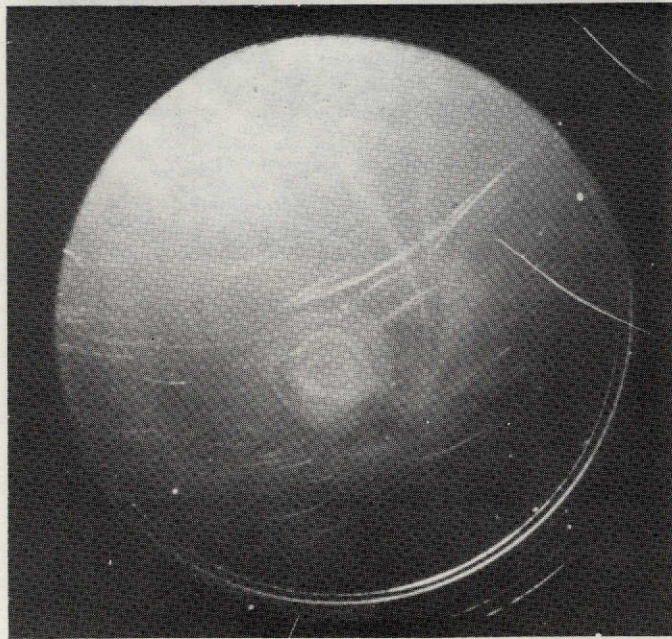


Figure 6. - Top view of flow without swirl observed in apparatus of figure 2.

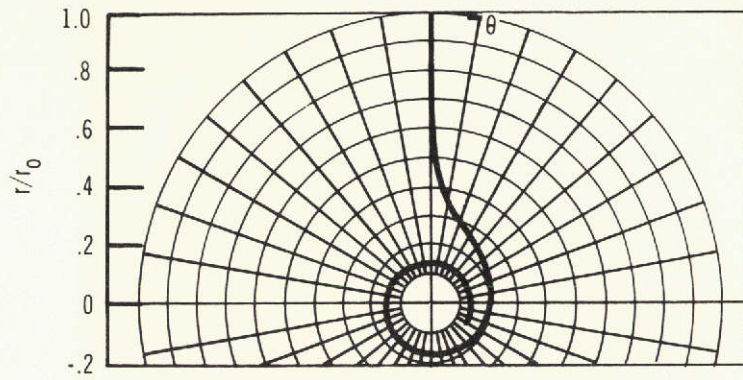


(a) Time, 0 second.

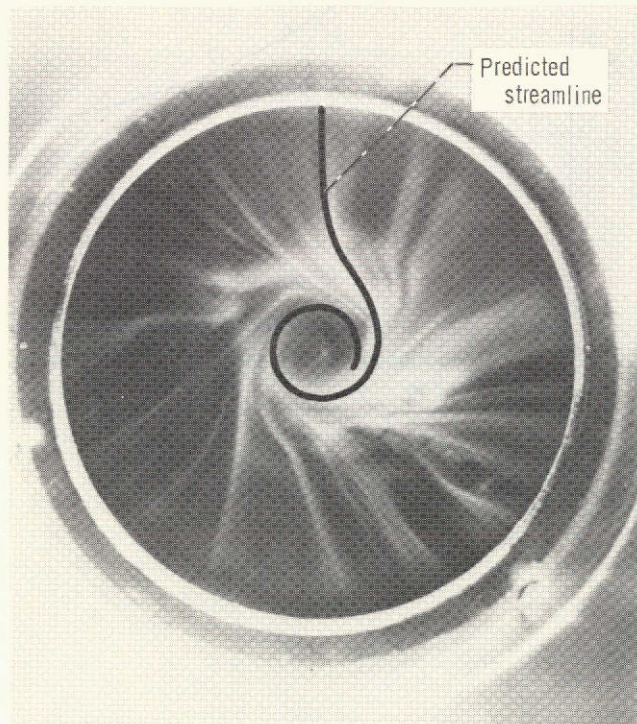


(b) Time, 0.8 second.

Figure 7. - Top view of vortex observed in apparatus of figure 2, but with horizontal plate at top of gap where fluid enters vortex region.



(a) Calculated from equation (16).



(b) Comparison of calculated streamline with experiment (fig. 3(f)).

Figure 8. - Top view of streamline.

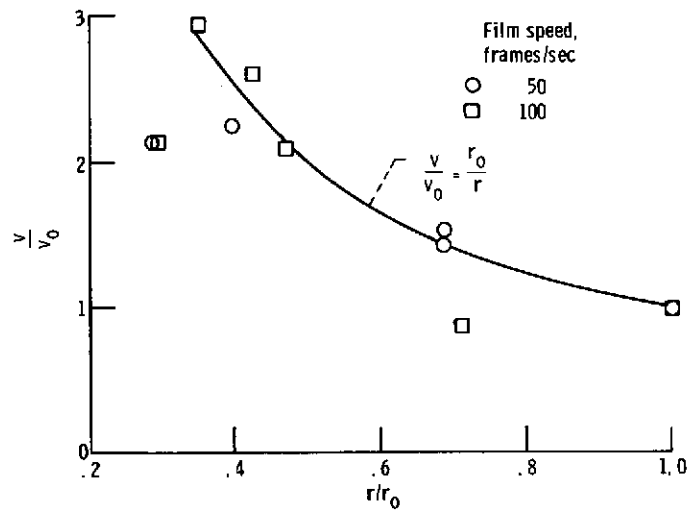


Figure 9. - Profile showing radial variation of tangential velocity.